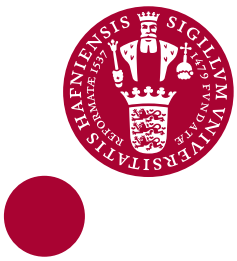

Profiling of G protein-coupled receptors in vagal afferents reveals novel gut-to-brain sensing mechanisms

Egerod, Kristoffer L.; Petersen, Natalia; Timshel, Pascal N.; Rekling, Jens C.; Wang, Yibing; Liu, Qinghua; Schwartz, Thue W.; Gautron, Laurent

Published in:
Molecular Metabolism

DOI:
10.1016/j.molmet.2018.03.016

Publication date:
2018

Document version
Publisher's PDF, also known as Version of record

Original Article

MOLECULAR METABOLISM

Profiling of G protein-coupled receptors in vagal afferents reveals novel gut-to-brain sensing mechanisms

Kristoffer L. Egerod [1,*], Natalia Petersen [1], Pascal N. Timshel [2], Jens C. Rekling [3], Yibing Wang [4], Qinghua Liu [4], Thue W. Schwartz [1], Laurent Gautron [5,]**

ABSTRACT

Objectives: G protein-coupled receptors (GPCRs) act as transmembrane molecular sensors of neurotransmitters, hormones, nutrients, and metabolites. Because unmyelinated vagal afferents richly innervate the gastrointestinal mucosa, gut-derived molecules may directly modulate the activity of vagal afferents through GPCRs. However, the types of GPCRs expressed in vagal afferents are largely unknown. Here, we determined the expression profile of all GPCRs expressed in vagal afferents of the mouse, with a special emphasis on those innervating the gastrointestinal tract.

Methods: Using a combination of high-throughput quantitative PCR, RNA sequencing, and *in situ* hybridization, we systematically quantified GPCRs expressed in vagal unmyelinated $Na_v1.8$-expressing afferents.

Results: GPCRs for gut hormones that were the most enriched in $Na_v1.8$-expressing vagal unmyelinated afferents included NTSR1, NPY2R, CCK1R, and to a lesser extent, GLP1R, but not GHSR and GIPR. Interestingly, both GLP1R and NPY2R were coexpressed with CCK1R. In contrast, NTSR1 was coexpressed with GPR65, a marker preferentially enriched in intestinal mucosal afferents. Only few microbiome-derived metabolite sensors such as GPR35 and, to a lesser extent, GPR119 and CaSR were identified in the $Na_v1.8$-expressing vagal afferents. GPCRs involved in lipid sensing and inflammation (e.g. CB1R, CYSLTR2, PTGER4), and neurotransmitters signaling (CHRM4, DRD2, CRHR2) were also highly enriched in $Na_v1.8$-expressing neurons. Finally, we identified 21 orphan GPCRs with unknown functions in vagal afferents.

Conclusion: Overall, this study provides a comprehensive description of GPCR-dependent sensing mechanisms in vagal afferents, including novel coexpression patterns, and conceivably coaction of key receptors for gut-derived molecules involved in gut-brain communication.

Keywords G protein-coupled receptors; Vagal afferent nerves; Gut-brain axis; Gut hormones; GLP1R; NTSR1

1. INTRODUCTION

The gastrointestinal (GI) mucosa has long been known to be richly innervated by unmyelinated axons [1,2]. These axons typically wander within the lamina propria, often approaching its epithelium without penetrating the basal lamina. While many axons present in the GI mucosa are of enteric origin [3], anterograde tracing studies revealed that vagal afferents also abundantly innervate the GI mucosa [4–8]. Some vagal unmyelinated afferents supplying the GI tract are polymodal [9], and electrophysiological studies have demonstrated that mucosal vagal afferents respond to a wide range of molecules absorbed across the epithelium or locally released, in addition to the distension of the alimentary canal, as well as noxious, thermic and osmotic stimuli [10–17]. Thus, it is not surprising that a variety of sensations and autonomic reflexes can be elicited by the mechanical or chemical stimulation of the GI mucosa [18–21].

Many of the molecules that modulate the activity of vagal afferents, including neurotransmitters, gut peptides, lipids, and metabolites, are G protein-coupled receptors (GPCRs) ligands [22]. However, due to a lack of understanding of GPCRs distribution in vagal afferents, it is unknown whether the aforementioned molecules directly act on these neurons. For instance, a prevalent view suggests that vagal GI mucosal afferents directly respond to peptides released from enteroendocrine cells including, cholecystokinin (CCK) and glucagon-like peptide 1 (GLP-1) [23–27]. In support of this view, the receptors for CCK and GLP-1 are abundantly expressed in vagal afferents [7,28–30], and

[1]Laboratory for Molecular Pharmacology, Department of Biomedical Sciences, and Novo Nordisk Foundation Center for Basic Metabolic Research, University of Copenhagen, Nørre Allé 14, 2200, Copenhagen, Denmark [2]Nordisk Foundation Center for Basic Metabolic Research, Section of Metabolic Genomics, Faculty of Health and Medical Sciences, University of Copenhagen, Nørre Allé 14, 2200, Copenhagen, Denmark [3]Department of Neuroscience, University of Copenhagen, Nørre Allé 14, 2200, Copenhagen, Denmark [4]Department of Biochemistry, UT Southwestern Medical Center at Dallas, The University of Texas Southwestern Medical Center, 5323 Harry Hines Blvd., Dallas, TX 75390, USA [5]Division of Hypothalamic Research and Department of Internal Medicine, The University of Texas Southwestern Medical Center, 5323 Harry Hines Blvd., Dallas, TX 75390, USA

*Corresponding author. E-mail: Egerod@sund.ku.dk (K.L. Egerod).

**Corresponding author. E-mail: Laurent.gautron@UTSouthwestern.edu (L. Gautron).

Received February 27, 2018 • Revision received March 24, 2018 • Accepted March 29, 2018 • Available online 3 April 2018

https://doi.org/10.1016/j.molmet.2018.03.016

CCK and GLP-1 acutely enhance the activity of vagal afferents [10,31]. Moreover, the anorectic effects of peripheral CCK and GLP-1 are attenuated in deafferented animals [32–35]. Despite these findings, several other studies have suggested that gut-derived CCK and GLP-1 act through potentiating vagal responses to distending loads and/or directly on the brain [36–40]. A recent study further challenged the common view that CCK and GLP-1 can be directly detected by mucosal afferents by demonstrating that neurons expressing receptors for these gut hormones do not innervate the mucosa [7]. Lastly, considering that at least 10 different peptides are known to be secreted by different types of enteroendocrine cells [41], it is unknown which gut peptides, other than CCK and GLP-1, can be detected by vagal afferents.

Here, we determine the expression profile of all GPCRs in the vagal afferents of the mouse. A special emphasis was given to vagal afferents expressing $Na_v1.8$, a voltage-gated sodium channel involved in the generation of action potentials in vagal unmyelinated afferents [16,42,43]. $Na_v1.8$-expressing vagal afferents richly innervate the entire GI mucosa [5], making these neurons ideally positioned to detect nutrients and molecules locally released in the GI tract. To better understand how the vast assortment of GPCRs contribute to vagal sensing mechanisms, we fully characterized GPCRs expression in $Na_v1.8$-expressing vagal afferents using a combination of quantitative PCR (qPCR), RNA sequencing, and double *in situ* hybridization studies.

2. MATERIALS AND METHODS

2.1. Mice

Male C57BL/6JRj and C57BL/6J wild-type mice were purchased from Janvier Breeding Centre (France) and the ARC at UT Southwestern Medical Center (Dallas), respectively. These mice were used for qPCR assays, chromogenic Brown, Red, and Duplex *in situ* hybridization.

$Na_v1.8$-Cre-DTA mice were generated and genotyped as previously described by us [44]. Briefly, we crossed $Na_v1.8$ knock-in Cre-recombinase mice (gift from Dr. John Wood, University College London) on a pure C57Bl/6J background with ROSA26-eGFP-DTA mice (stock #006331; The Jackson Laboratory, USA) to generate litters with a 1:1 ratio of littermate controls ($Na_v1.8$-Cre) and ablated mice ($Na_v1.8$-Cre-DTA). Young male ablated and control mice were used for RNA-Seq studies.

$Na_v1.8$-Cre-ChR2-YFP male mice were also used for the purpose of ISH combined with immunohistochemistry. Mice carrying one $Na_v1.8$-Cre and one ChR2-YFP alleles were generated and genotyped exactly as previously described by us [45]. In these mice, YFP clearly delineates the membrane of $Na_v1.8$ neurons, hence facilitating double labeling analysis.

All mice used were young males (6–10 weeks old) housed in a barrier facility with temperature controlled environment (~23 °C). Mice were fed *ad libitum* with standard chow. The Danish Animal Experiments Inspectorate or Institutional Animal Care and Use Committee at the University of Texas Southwestern Medical Center at Dallas approved all animal procedures.

2.2. qPCR array of nodose ganglia

Wild-type mice (C57/Bl6JRj, Janvier) were euthanized using cervical dislocation and the nodose ganglia from 2 mice were dissected into RNAlater at room temperature and kept at 4°C overnight prior of RNA extraction using the NucleoSpin® RNA XS (MACHEREY-NAGEL) and RT-PCR was performed using SuperScript III Reverse Transcriptase (Invitrogen). Custom-designed RT2 Profiler PCR Arrays (Qiagen) was used to analyze 377 GPCRs and 3 Receptor-Activity Modifying Proteins (RAMPS) on a LightCycler480 (Roche). Relative expression was calculated using the formula:

$$Relative\ expression = 2^{-(CqTarget - CqRef)} \times C$$

where CqTarget = the quantification cycle (Cq) for the target gene; CqRef = the geometrical mean of the quantification cycle for the reference genes (Ywhas, Actb and Gapdh); C is an arbitrary constant dependent on CqRef used to shift the relative expression so Cq values of 35 on average are equal to 1, here C = 24221. Undetectable targets were assigned a Cq value of 40. In total 8 mice was used to generate the 4 samples analyzed. Information of genes on the qPCR array is given in Table S1.

2.3. RNA-sequencing of nodose ganglia

RNA sequencing was performed on the nodose ganglia of ablated and control mice (n = 3/group). The two nodose ganglia (left and right) from one mouse were pooled and RNA was extracted as described above for qPCR. Library construction (Truseq, Illumina), sequencing (Hiseq 100 PE, Illumina) and read quality control filtering was performed at BGI Tech solutions (Hong Kong). The sequencing data was processed using the "Tuxedo tools" (Tophat2, Cufflinks2, cummeRbund) as outlined in [46] using the mm10 reference annotation only. Briefly, normalized expression quantification and differential expression tests for Ensembl genes were obtained using Cuffdiff2 with "–frag-bias-correct" [47] and "–multi-read-correct" enabled. The output from Cuffdiff2 [46] was analyzed with the R package cummeRbund (version 2.12.1).

2.4. *In situ* hybridization

2.4.1. RNAScope chromogenic "brown" assay

Wild-type mice received an overdose of chloral hydrate (500 mg/kg, i.p.) and their nodose ganglia were rapidly dissected and frozen on dry ice. Ganglia were cut using a cryostat at 14 μm and stored at −80 °C. Following the manufacturer's protocol (Advanced Cell Diagnostic), ganglia were hybridized with double-Z oligo probes for the genes listed in Table S2. Signal detection was achieved using DAB and tissue was counterstained with Nuclear Fast Red (Sigma).

2.4.2. RNAScope chromogenic "red" assay combined with immunohistochemistry for YFP

$Na_v1.8$-Cre-ChR2-YFP mice were anesthetized with chloral hydrate (500 mg/kg, i.p.) and transcardiacally perfused with 10% formalin (Sigma). Fixed nodose ganglia were kept in 10% formalin for 48 h at 4 °C before being transferred into 20% sucrose in PBS for an additional 24 h. Ganglia were next frozen and cut at 14 μm onto SuperFrost Plus slides (1:5 series). Tissue was baked at 60 °C for 30 min, washed in 1X PBS, treated in H_2O_2 for 10 min. Pretreatment consisted of hot 1X Target Retrieval solution for 1–2min. Next, slides were rinsed in distilled water and dehydrated in fresh 100% ethanol. Tissue was incubated with Pretreatment 3 at 40 °C for 15mins. After rinsing the slides in distilled water, hybridization was performed using the standard ACD procedure and reagents from the RNAscope® 2.5 HD Detection Kit (RED). The probes listed in Table S2 were applied at 40 °C for 2hrs. Amplification steps were done using the following the manufacturer's instructions. Lastly, signal detection was achieved using a mix of Fast RED-B and Fast RED-A in a ratio of 1:60 at room temperature for about 10 min. Slides were washed in distilled water. The native tdTomato fluorescence was greatly diminished following *in situ* hybridization. Nodose ganglia were next labeled using a GFP

chicken antibody known to detect YFP (1:1,000). On the next day, tissue was rinsed and incubated in a solution of biotinylated anti-chicken (1:1,000; Cat#703065155; Jackson ImmunoResearch) for 1hr, followed by Streptavidin, AlexaFluor 488 (1:1,000; Cat#S32354; Invitrogen) for 1 h. EcoMount mounting medium was applied to the slides and coverslip over the tissue section. Pilot experiments in adjacent tissue sections were also performed to ensure that the combination of *in situ* hybridization with immunohistochemistry did not alter the staining obtained with each individual procedure.

2.4.3. RNAScope chromogenic "duplex" assay

Fixed nodose ganglia were obtained from C57Bl/6J mice as described for the "red" assay. Ganglia were next frozen and cut at 8 μm onto SuperFrost Plus slides (1:5 series). Tissue was pretreated with boiling 1X Target Retrieval followed by Protease III at 40 °C for 15mins. After pretreatment, the slides were hybridized with the probes listed in Table S2. Amplification steps were done using the reagents from the RNAscope® 2.5 HD Duplex Assay. Signal detection was achieved using two different chromogenic substrates (HRP-C1-Green and AP-C2-Red). Finally, slides were counterstained with hematoxylin and covered with EcoMount mounting medium.

As a negative control, we used a probe recognizing the prokaryotic gene dapB. Ganglia were completely devoid of a signal. As a positive control, we detected the expression of cyclophilin mRNA across the nodose ganglion (data available upon request).

2.4.4. Microscopy

Images of DAB- and Duplex-labeled ganglia were captured using the standard brightfield optics of a Zeiss Axioplan light microscope attached to a digital camera. Images of FastRed-labeled ganglia were acquired using the 63x oil objective of the Leica Sp5 confocal laser scanning microscope (UT Southwestern Live Imaging Core Facility). Estimates were performed using ImageJ. Specifically, we manually counted YFP-positive cells expressing select receptors and expressed the data as percentage of Nav1.8 coexpression. This was done in 2–4 left ganglia from different mice. For each gene, we counted a total of 262–536 cell profiles. Data were expressed as the percentage of YFP-positive cell profiles expressing red dots. In Duplex-labeled ganglia, we counted the number of neuronal profiles unequivocally containing green and/or red dots in 2–3 left ganglia from different mice. For each combination of gene, we counted a total of 215–572 cell profiles. Data were included in pie charts representing the percentage of cell profiles expressing green, red, or both green and red dots. Lastly, Adobe Photoshop CS5 was used to annotate, crop and adjust the contrast of our digital images.

2.5. Patch clamp on ex vivo cultures of vagal afferent neurons

Mice were euthanized by cervical dislocation, and the ganglia was dissected into DMEM (Dulbecco's Modified Eagle Medium) at 4 °C. For a typical experiment, ganglia from 4 mice were pooled prior of incubation at 37 °C in DMEM supplemented with 1.3 Wünsch units/ml Liberese TM (Roche) for ~1 h. During the first half hour, the tubes were shaken every 10 min. The next half hour, the samples were resuspended using a pipette every 10 min. After 1 h, the samples were resuspended using a pipette every 5 min until the sample was clearly digested and the majority of cells in single cell suspension. The cells were passed through a cell strainer (70 μm) and resuspended in DMEM. The cell suspension was distributed on poly-D-lysin coated coverslips and cultured during 4–6 days in Neurobasal Medium (Gibco) containing 100 units/mL penicillin/streptomycin, 10 mmol/L HEPES, 2 mmol/L Glutamax and B27 supplement (Gibco). On day two, the cultures were treated with 0.5 μM Ara-C in the culture medium for 48 h to eliminate glial cells. For electrophysiological measurements, the neurons on coverslips were transferred to a 1 ml recording chamber and superfused at room temperature with an artificial ganglion solution (AGS) containing (in mM): 152 NaCl, 5 KCl, 10 HEPES, 10 D-Glucose, 1 MgCl2, 2 CaCl2 with a pH of 7.4. Whole-cell patch clamp recordings were performed in current clamp using an AxoClamp 2B amplifier (Molecular Devices, Sunnyvale, CA, USA). Data were digitally acquired at a sampling rate of 10 kHz. Glass micropipettes were pulled from filament capillary glass (O.D. 1.5 mm, I.D. 0.86 mm, Harvard Apparatus, Holliston, MA, USA) using a PUL-100 micropipette puller (World Precision Instruments, Sarasota, FL, USA) to a tip resistance of 4–6 MΩ. Patch pipettes were filled with a solution containing (in mM): 130 HCH3SO3, 130 KOH, 10 HEPES, 0.4 NaGTP, 4 Na2ATP, 5 Na2-phosphocreatine, 4 MgCl2, whose osmolarity measured 310 mOsm with a pH of 7.3. Patch pipettes were visually guided to target tdTomato-positive neurons under visual control using ROE-200 micromanipulators (Sutter Instruments, Novato, CA, USA) on a fixed-stage upright microscope (modified Olympus BX51, Olympus Corporation, Tokyo, Japan) under 40X magnification. Local application of CCK (50 nM dissolved in 50% water, 50% AGS) was done by placing a separate patch pipette close to the cell and applying 5–25 psi pressure for 5 – ~60 s. Electrophysiological data was acquired using pClamp 10.0 (Molecular Devices, Sunnyvale, CA, USA) and subsequently analyzed using Igor Pro 7 (Wavemetrics, Tigard, OR, USA).

3. RESULTS

3.1. $Na_V1.8$ neurons ablated mice lack unmyelinated vagal afferents

Receptors enriched in $Na_V1.8$-expressing vagal afferents were identified by comparing the transcriptional profile of nodose ganglia from mice lacking $Na_V1.8$ neurons (ablated) to that of control littermates. Successful ablation of $Na_V1.8$ neurons in $Na_V1.8$-Cre-DTA mice was previously demonstrated by us and others [44,48]. RNAseq comparison of the nodose ganglion of ablated and control mice further revealed very little expression of several markers selective of unmyelinated peptidergic and non-peptidergic sensory neurons, including *$Na_V1.8$*, *Trpa1*, *Trpv1*, *Sst*, and *Plxnc1* (Figure S1) [49] in the ablated mice. With the exception of *Cacna1h*, all genes enriched in myelinated neurofilament-containing afferents including *Nefh*, *Trkb*, and *Spp1*, in ablated animals (Figure S1) [49]. Several genes such as *$Na_V1.9$*, *Calca*, and *Tac1* showed reduced expression in ablated mice (Figure S1). Their residual expression in ablated mice could be attributed to their expression in small subtypes of myelinated neurons [49]. The expression of several neuropeptides appeared downregulated in the nodose ganglion of ablated mice including *Sst*, *Calca*, *Calcb*, *Nmb* and *Pcart* (Figure S1). Overall, we confirmed that ablated mice showed a selective lack of unmyelinated vagal afferents including many peptidergic neurons. In the following sections, we characterized the change in expression of GPCRs in afferent vagal neurons upon $Na_V1.8$ ablation.

3.2. A group of selected gut peptide receptors are expressed in vagal afferents

It is well established that a major part of the effects of certain gut hormones such as CCK and GLP-1 is mediated through afferent vagal signaling [10,26,27,31]. However, the expression of peptide receptors and their subtypes has not been systematically studied. As shown in Figure 1A, qPCR of the whole nodose ganglion revealed that the expression profile was dominated by *Cck1r*, *Glp1r*, *Npy2r*, and *Ntsr1*. These receptors are conceivably sensing gut-derived CCK, GLP-1, PYY,

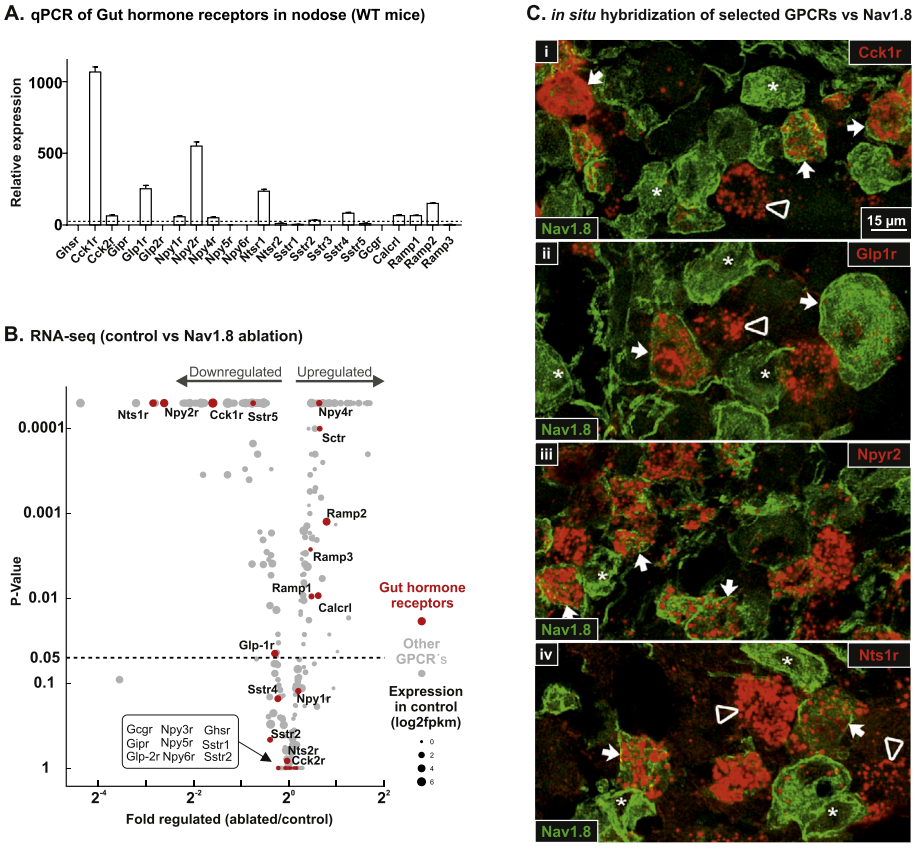

Figure 1: Gut hormone receptors expression and enrichment in $Na_V1.8$-expressing vagal afferents. (A) Expression level of gut hormone receptors in vagal afferent (whole nodose ganglion) of wild-type (WT) mice, the dotted line indicates the median for GPCRs expression. (B) Volcano plot for the fold change of expression level for 408 GPCRs (gray dots) in $Na_V1.8$ neurons ablated vs. control mice. Gut hormone receptors are shown in red with corresponding names, the size of the dots relate to the expression level prior of ablation. (C) *In situ* hybridization of selected gut hormone receptors (i; Cck1r, ii; Glp1r, iii; Npyr2 and iv; Ntsr1) in red vs. immunohistochemical detection of YFP in the nodose ganglion of $Na_V1.8$ reporter mice ($Na_V1.8$-Cre-ChR2-YFP) in green. Asterisks indicate representative $Na_V1.8$ positive cells. Triangles and arrows indicate examples of gut hormone receptor positive cells and double positive cells, respectively.

and neurotensin. Other receptor subtypes for these ligands including *Cck2r*, *Npy1*,*4-6r*, and *Ntsr2* were only expressed at a low level. The *Sstr4* somatostatin receptor was expressed above noise level. Interestingly, the GIP receptor *Gipr* was expressed below the detection limit, thus suggesting that GIP does not exert its function through afferent vagal neurons. Likewise, the expression of the ghrelin receptor, *Ghsr* was also below detection limit in the nodose ganglion, thereby challenging previous reports that certain effects of these hormones are dependent upon vagal sensory signaling [50–52]. In support of our data, accumulating evidence indicates that only hypothalamic neurons are required for the orexigenic actions of ghrelin [53–55].

As shown above, $Na_V1.8$ ablated mice show a selective loss of unmyelinated vagal afferents. Below, we characterized the changes in expression of GPCRs in the nodose ganglion upon $Na_V1.8$-expressing cells ablation. *Ntsr1*, *Npy2r*, and *Cck1r* were highly enriched in $Na_V1.8$ neurons as judged by their large reduction in expression upon ablation (Figure 1B). *Npy2r* and *Ntsr1* were the most downregulated in ablated animals, indicating their nearly exclusive expression in $Na_V1.8$ cells (Figure 1B). The enrichment was further validated using ISH combined with immunohistochemistry in reporter mice for $Na_V1.8$ neurons ($Na_V1.8$-Cre-ChR2-YFP) [45]. For instance, *Npy2r* and *Ntsr1* were expressed in 71% and 40% of $Na_V1.8$ cells, respectively (Figure 1C). In comparison, *Cck1r* was enriched in a large proportion of $Na_V1.8$ cells (42%) but was not restricted to $Na_V1.8$ cells (Figure 1C). In contrast, *Glp1r* was only slightly and only barely significantly affected by the ablation (Figure 1B). Double ISH demonstrated that *Glp1r* was expressed in only 18% of $Na_V1.8$ afferents (Figure 1C). Moreover, about half of *Glp1r*-expressing afferents were $Na_V1.8$-negative (52%) and appeared to express higher levels of *Glp1r* mRNA (Figure 1C).

Functional CCK_1 receptor was further validated through whole-cell patch clamp performed on isolated neurons from the nodose. The neurons showed typical electroresponsive properties of nodose ganglion neurons, i.e. single or dual spikes in response to a prolonged depolarizing current pulse (Figure S2). Pressure application of CCK (50 nM) from a separate patch pipette positioned close to the neuron depolarized a subset of neurons 9–38 mV (4 responders, 15 non-responders), accompanied by an increase in the membrane noise and shunting of the membrane. Repeated pressure application to responders resulted in desensitization of the depolarizing response ($n = 3$).

Overall, vagal unmyelinated afferents were found to be enriched in the receptors for only a few select gut peptides.

3.3. NTSR1 is the only gut peptide receptor preferentially expressed in mucosal afferents

Because $Na_V1.8$-expressing vagal afferents do not exclusively innervate the GI mucosa, but also the GI muscularis and several other peritoneal and thoracic organs [5], we judged it necessary to further

narrow down the identity of vagal afferents enriched with gut peptide receptors. Specifically, we used double *in situ* hybridization studies with *Cck1r* and *Gpr65*, which identify non-overlapping population of vagal afferents preferentially innervating the GI muscularis and mucosa, respectively [56]. Here, we confirmed that very few neurons coexpressed *Cck1r* and *Gpr65* in the nodose ganglion (Figure 2A). Importantly, about half of the *Cck1r*-expressing neurons also expressed *Glp1r* and almost all *Glp1r* neurons were positive for *Cck1r* (Figure 2B), whereas *Glp1r* like *Cck1r* almost never colocalized with *Gpr65* (Figure 2C). These data are in agreement with the view that *Cck1r*- and *Glp1r*-enriched vagal afferents represent a mixed population of unmyelinated and myelinated fibers innervating the GI muscularis rather than its mucosa [56]. More than half of the *Cck1r*-expressing neurons also expressed *Npy2r* (Figure 2D). This is surprising considering that *Npy2r* neurons were previously described as unmyelinated neurons innervating the lungs [57]. Nonetheless, we also found that many *Npy2r* neurons neither express *Cck1r* nor *Gpr65* (Figure 2E), presumably corresponding to pulmonary vagal afferents.

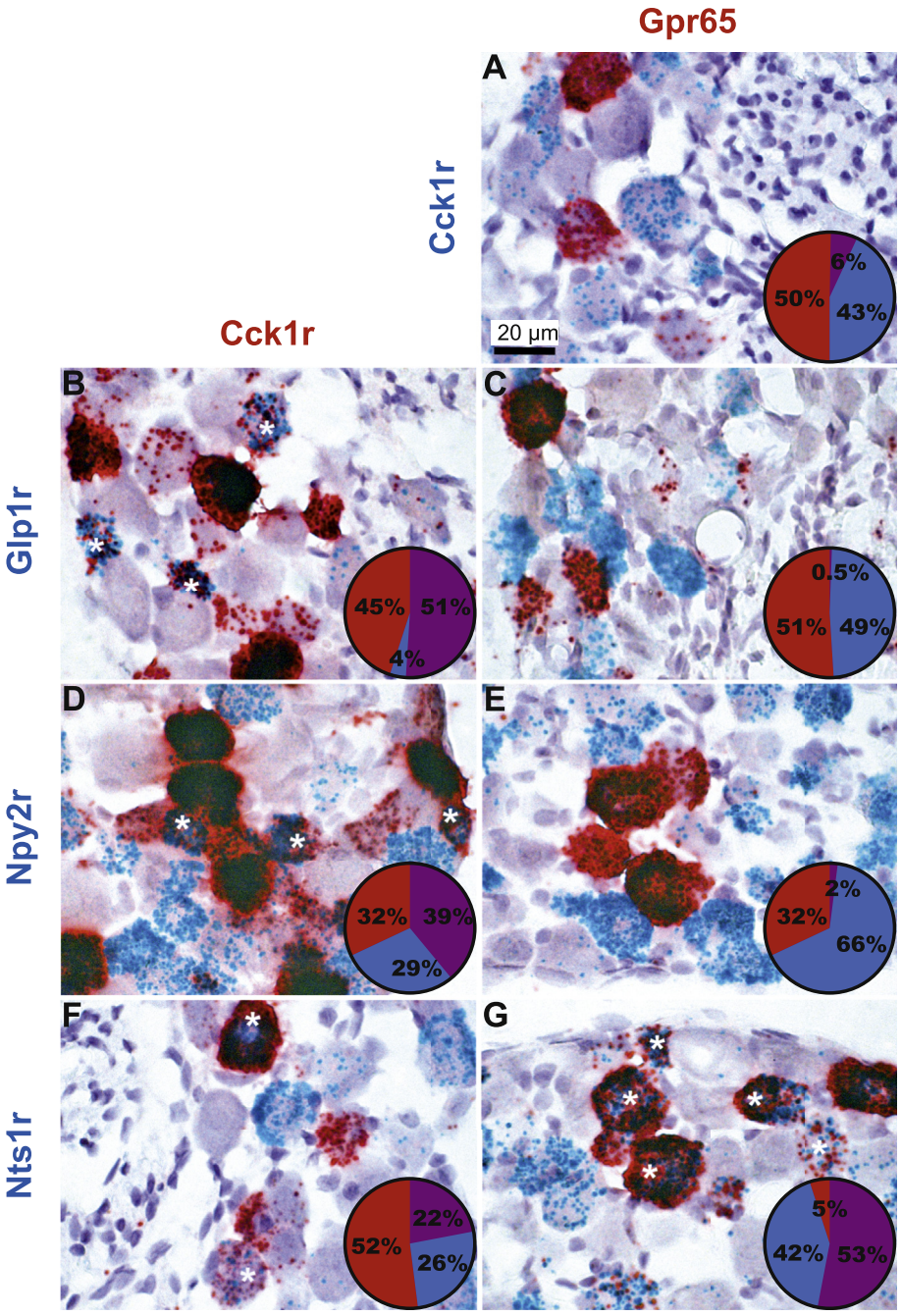

Figure 2: Double chromogenic *in situ* hybridization for gut hormone receptors. A, C, E, and G *in situ* hybridization for Gpr65 in red vs. Cck1r, Glp1r, Npy2r, or Ntsr1 in blue. B, D, F *in situ* hybridization for Cck1r in red vs. Glp1r, Npy2r, orNtsr1 in blue. Asterisks indicate representative double-labeled cell profiles. Pie charts give the percentage of single positive cells (red or blue) and double positive cells (purple). Bright-field images were collected from the nodose ganglion of wild-type mice. Tissue was counterstained with hematoxylin.

Interestingly, nearly all *Gpr65*-expressing neurons expressed *Ntsr1* (Figure 2G), which also was expressed in ~25% of the *Cck1r*-neurons (Figure 2F). Neurotensin is normally co-secreted from enteroendocrine cells with GLP1 and PYY in response to metabolic stimuli [58]. Our data imply that neurotensin may act in a paracrine manner on vagal unmyelinated afferents innervating the intestinal mucosa.

3.4. Only few receptors for microbial metabolites are expressed in vagal afferents

A number of GPCRs function as sensors of diet-derived, nutrient metabolites, and metabolites generated by the gut microbiota [22]. Whereas these metabolite receptors are known to be expressed on enteroendocrine cells, their neuronal expression has not been systematically studied. As shown in Figure 3, only 4 metabolite receptors were expressed above background in the nodose ganglion. Specifically, *Gpr119*, *Ffar3* (*Gpr41*), and *CaSR* were detectable in the whole nodose ganglion but at relatively low levels (Figure 3A). To our knowledge, only FFAR3 was previously described in vagal afferents [59,60]. In agreement with those studies, both qPCR and chromogenic ISH revealed that the short chain fatty acid receptor *Ffar3* was expressed at low level in very few cells (Figure S3) Interestingly, *Ffar3* was not down-regulated in $Na_V1.8$ ablated mice (Figure 3B). The calcium-sensing receptor (*CaSR*) and *Gpr119* were both expressed only a little higher than the median (Figure 3A) and were only moderately decreased upon $Na_V1.8$ ablation (Figure 3B). ISH for *Gpr119* mRNA confirmed very low levels of expression in the nodose ganglion compared to other receptors (Figure S3). GPR35, a receptor for aromatic, acidic metabolites such as the Trp metabolite kynurenic acid was the most highly expressed metabolite receptor and one of the most highly enriched GPCRs in $Na_V1.8$ neurons according to the more than 100-fold downregulation upon ablation (Figure 3A). Double chromogenic *in situ* hybridization further demonstrated that *Gpr35* was often coexpressed with *Cck1r* and almost all of the gastrointestinal mucosa innervating GPR65 expressing neurons (Figure 3C).

3.5. CB1R and several inflammatory lipid receptors are highly expressed in vagal afferents

GPCRs also act as molecular sensors of lipophilic hormones and lipids [22]. Dietary lipids, prostaglandins, and endocannabinoids were reported to acutely enhance the electrophysiological activity of vagal afferents [61–63]. However, little is known about the mechanisms underlying lipids sensing in vagal afferents. Here, we found that a large number of lipid receptors were highly expressed in the whole nodose ganglion (Figure 4A) and, furthermore, enriched in many $Na_V1.8$-expressing cells (Figure 4B). These receptors included *Cb1r*, *S1pr3*, *Lpar5*, and several prostaglandin receptors such as *Ptger4*, *Ptger1*, *Ptgir*, *Ptgdr*, *Ptger1*, *Ptgir*, and *Prgdr* were moderately enriched in $Na_V1.8$ cells (Figure 4B). *In situ* hybridization revealed that for instance

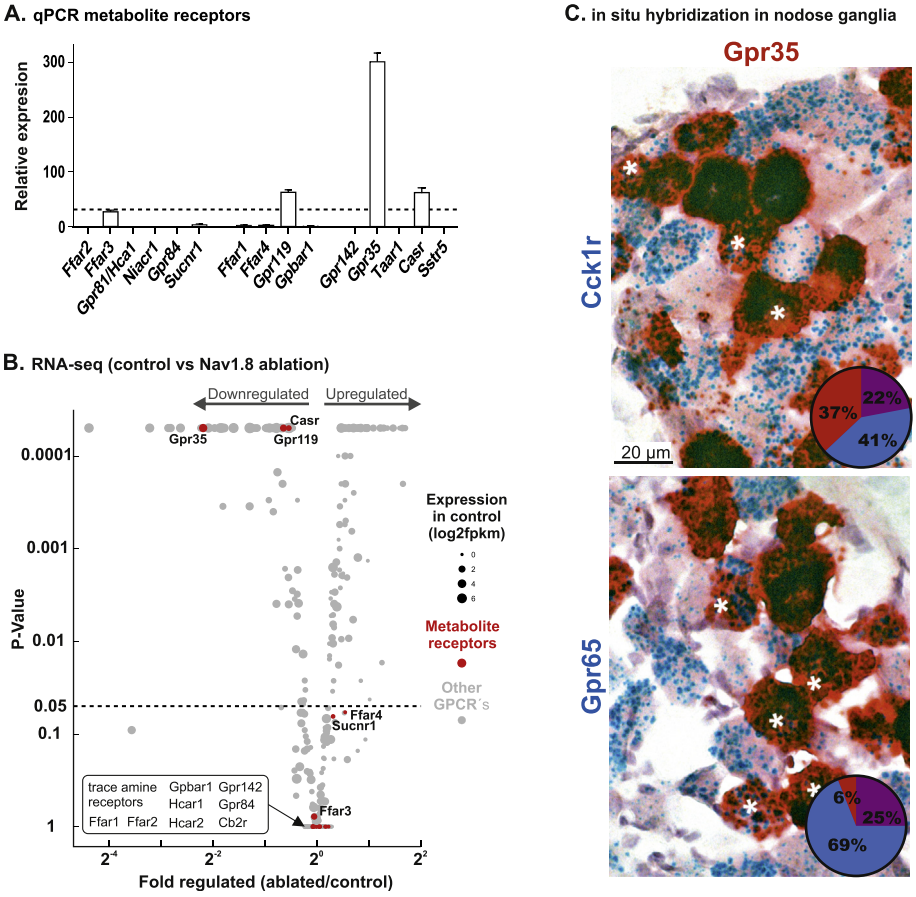

Figure 3: Metabolite receptors expression and enrichment in $Na_V1.8$-expressing vagal afferents. (A) Expression level of metabolite receptors in vagal afferents (whole nodose ganglion) of wild-type (WT) mice. The dotted line indicates the median for GPCRs expression. (B) Volcano plot for the fold change of expression level, for 408 GPCRs (gray dots) in $Na_V1.8$ neurons ablated vs. control mice. Metabolite receptors are shown in red with corresponding names, the size of the dots relate to the expression level prior of ablation. (C) *in situ* hybridization for Gpr35 in red vs Cck1r and Gpr65 in blue. Pie charts give the percentage of single positive cells (red or blue) and double positive cells (purple).

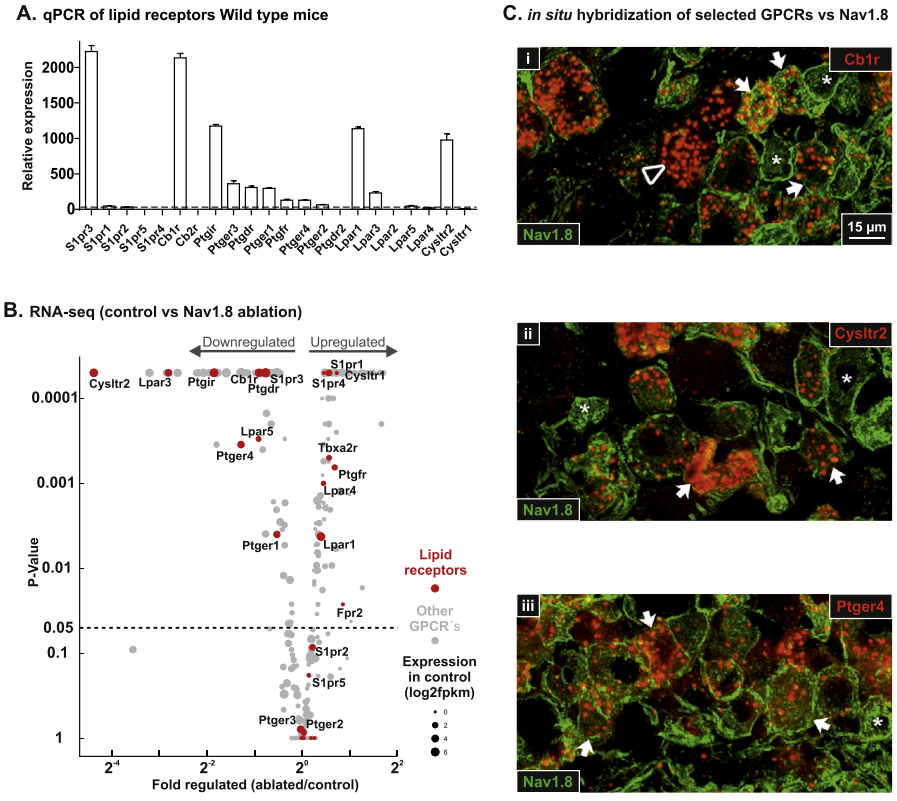

Figure 4: Lipid receptors expression and enrichment in $Na_V1.8$-expressing vagal afferents. (A) Expression level of lipid receptors in vagal afferent (whole nodose ganglion) of WT mice, the dotted line indicates the median for GPCRs expression. (B) Volcano plot for the fold change of expression level for 408 GPCRs (gray dots) in $Na_V1.8$ neurons ablated vs. control mice. Lipid receptors are shown in red with corresponding names, the size of the dots relate to the expression level prior of ablation. (C) *In situ* hybridization of selected lipid receptors (i; Cb1r, ii; Cysltr2, iii; Ptger4) in red vs. immunohistochemical detection of YFP in the nodose ganglion of $Na_V1.8$ reporter mice ($Na_V1.8$-Cre-ChR2-YFP) in green. Asterisks indicate representative $Na_V1.8$ positive cells. Triangles and arrows indicate examples of lipid receptor positive cells and double positive cells, respectively.

the cannabinoid receptor *Cb1r* was detected in ~65% of $Na_V1.8$ cells, but also in other neurons (Figure 4C). Thus, these receptors were not limited to the $Na_V1.8$ positive vagal afferents. In contrast, other lipids receptors were almost exclusively expressed in $Na_V1.8$ cells. These included *Ptge4*, *Cysltr2*, and *Lpar3*. For instance, *Cylstr2* and *Ptger4* were detected in 41% and 88% of $Na_V1.8$ cells (Figure 4C), respectively, and no other cells.

We verified the expression of select highly enriched lipid receptors in Cck1r and Gpr65-expressing neurons using double chromogenic *in situ* hybridization. As a result, we found that *Cysltr2*, and *Ptger4* were coexpressed with the vast majority of *Gpr65* neurons and a large subset of *Cck1r* neurons (Figure 5A—D). *Cb1r* was even more broadly expressed in almost all *Cckar*- and *Gpr65*-expressing neurons (Figure 5E,F). In summary, vagal unmyelinated afferents supplying the GI tract were found to be highly enriched in many receptors for immunomodulatory lipids and endogenous cannabinoids.

3.6. Multiple orphan GPCRs are broadly expressed in vagal afferents

Unexpectedly, we identified at least 21 orphan receptors that were highly enriched in the whole nodose ganglion and enriched in $Na_V1.8$ neurons (Figure 6A,B). For the majority of these receptors, their function(s) in neuronal signaling is unknown and never described before in vagal afferents. The most highly expressed orphan receptor was *Gpr149* (Figure 6A). In agreement with a recent study [56], we observed a high expression of *Gpr65* in the nodose ganglion. Importantly *Gpr65* was the second most down regulated GPCR upon Nav1.8 ablation (Figure 6A,B), indicating that this receptor normally is highly enriched in $Na_V1.8$-expressing vagal afferents. Here, we further showed using *in situ* hybridization that *Gpr65* is present in about 35% of $Na_V1.8$ cells and is not detectable in $Na_V1.8$-negative cells (Figure 6C). As discussed previously, *Gpr65* is a marker for GI mucosal afferents of unknown functions [56].

Many other orphan receptors (*Gpr174*, *Gpr161*, *Gpr158*, *Gpr160*, *Mrgprb4*, *Mrgprx1*, *Gpr22*) appeared highly expressed in the nodose ganglion and significantly down regulated in ablated mice (Figure 6A,B). *In situ* hybridization validated that, among these receptors, the orphan receptor *Gpr161* is expressed in almost all (97%) of the $Na_V1.8$ neurons (Figure 6C).

3.7. Receptors for classic neurotransmitters and neuropeptides

Numerous neurotransmitters of enteric or epithelial origins are released in the GI mucosa [64]. Our studies revealed that *Gabbr1* encoding the non ligand-binding protomer of the GABA dimeric receptor was very highly expressed in the nodose ganglion (Figure 7A,B). *In situ* hybridization confirmed its high expression level and nearly ubiquitous distribution across vagal afferents (Figure S3). The *Grm7* glutamate receptor was also ubiquitously expressed at relatively high level in vagal afferents (Figure 7A,B). Interestingly, the *Drd2* dopamine and *Chrm4* muscarinic acetylcholine receptor were both enriched in $Na_V1.8$ neurons (Figure 7B). For instance, *Drd2* was detected in about 43% of $Na_V1.8$ cells (Figure 7C). Interestingly, both *Drd2* and *Chrm4*

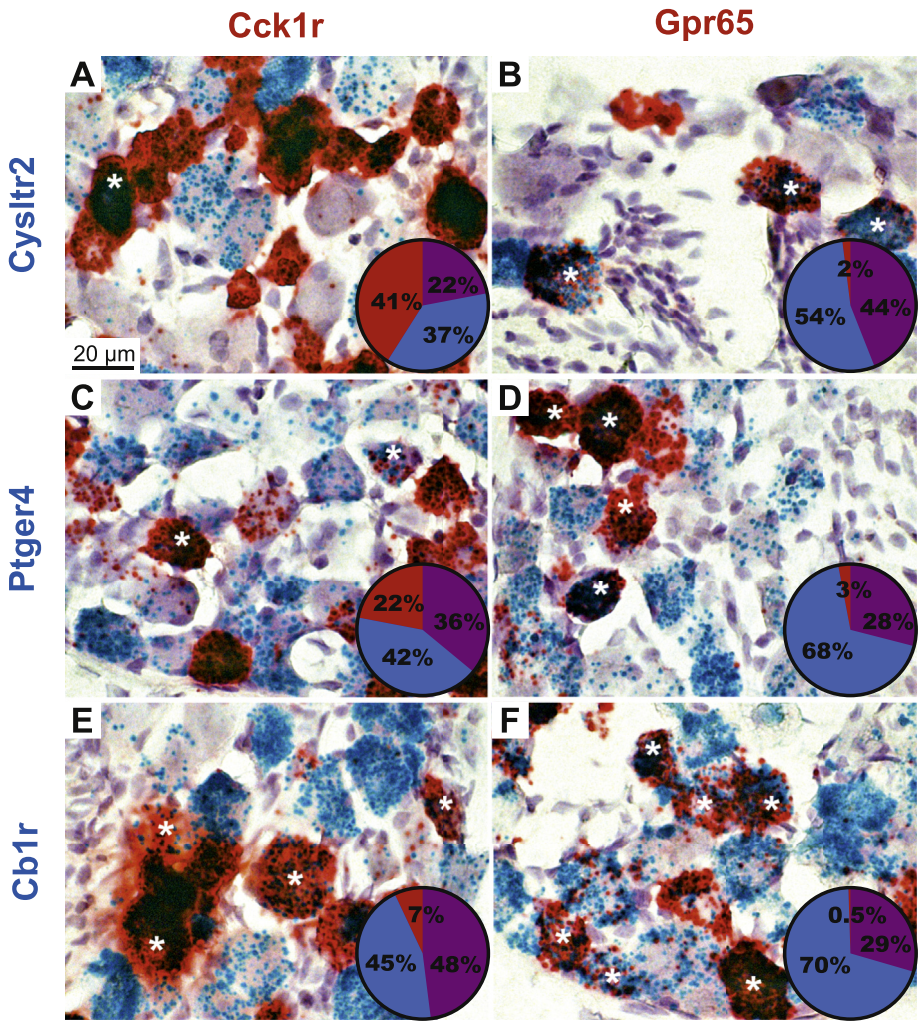

Figure 5: Double chromogenic *in situ* hybridization of lipid receptors. A, C, and E *in situ* for Cck1r in red vs. Cysltr2, Ptger4, Cb1r in blue. B, D, and F *in situ* for Gpr65 (a marker for gastrointestinal mucosa) in red vs. Cysltr2, Ptger4, Cb1r in blue. Asterisks indicate representative double-labeled cell profiles. Pie charts give the percentage of single positive cells (red or blue) and double positive cells (purple). Bright-field images were collected from the nodose ganglion of wild-type mice. Tissue was counterstained with hematoxylin.

were often coexpressed with *Cck1r*, but rarely with *Gpr65* (Figure 7D). Several serotonin receptors were also identified in $Na_v1.8$ cells (Figure 7A,B), which is interesting as 5-HT is produced from enterochromaffin cells, which constitute the largest population of enteroendocrine cells of the GI tract. Serotonin signaling via 5-HT3 in vagal afferents has been studied in the past [11,56], but the action of other neurotransmitters is poorly documented. Our data demonstrate that the sensitivity of vagal afferents to classic neurotransmitters is not limited to serotonin but likely extends to acetylcholine, glutamate, GABA, and dopamine.

Among receptors for neuropeptides, *Crhr2*, a receptor for corticotropin-releasing factor, was the most highly expressed in the whole nodose ganglion and highly enriched in $Na_v1.8$ cells (Table S1 and Figure S4). Roughly 75% of $Na_v1.8$ neurons were found to express *Crhr2* mRNA (Figure S4). Using double *in situ* hybridization, it was further shown that *Crhr2* colocalized with roughly one third of *Cck1r*- and half of *Gpr65*-expressing neurons (Figure S4). Since *Crhr2* binding sites are prominent in the nucleus of solitary tract [65], it is likely that *Crhr2* may serve as a presynaptic receptor on vagal terminals. Hence, it is tempting to speculate that *Crhr2* signaling in gastrointestinal vagal afferents may link stress to the regulation of satiety. Other receptors for neuropeptides were also enriched in vagal afferents including *Kiss1r* and *Opmr1* (Table S1). However, these receptors were moderately enriched in the nodose ganglion compared to Crhr2.

3.8. Additional receptors

The expression profile for GPCRs measured by qPCR and RNA-seq are given in Table S1. A few other noteworthy receptors that were highly enriched in vagal $Na_v1.8$ cells included receptors not known to be involved in gut-to-brain communication such as *F2r*, *Ackr4* and *Ednra* (Table S1 and Figure S5). The function of these receptors in neurons remains largely undocumented.

4. CONCLUSIONS AND PERSPECTIVES

Our current understanding of the molecular mechanisms through which microbial, neuronal, metabolic, and immune signals released in the gut influence vagal functions and thereby signaling to the brain and how these signals interact with each other remains incomplete. In the past, transcriptional profiling studies for GPCRs through which such

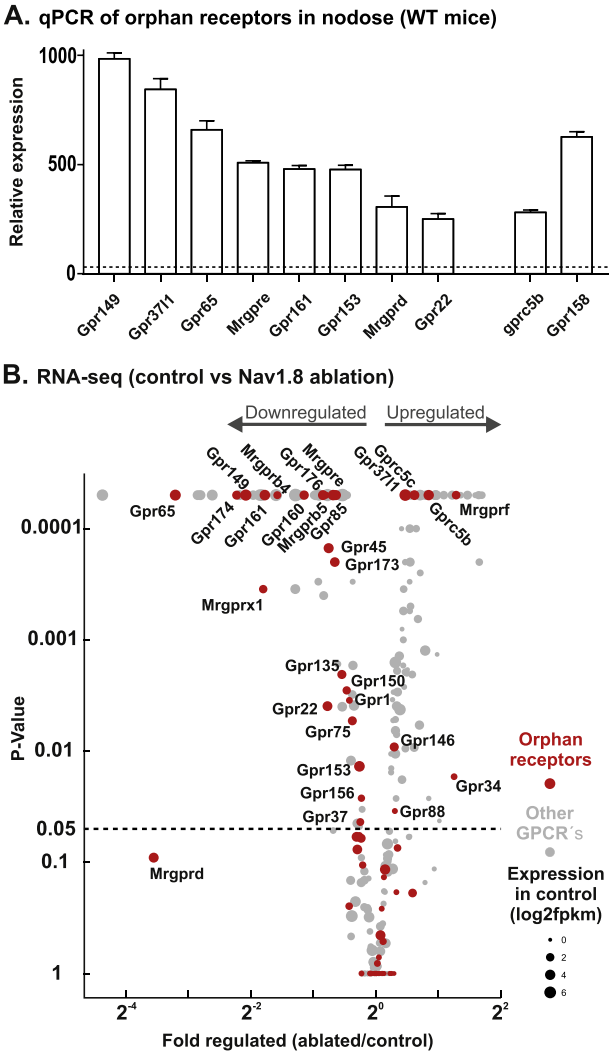

Figure 6: Orphan receptors expression and enrichment in $Na_V1.8$-expressing vagal afferents. (A) Expression level of selected orphan receptors in vagal afferent (whole nodose ganglion) of wild-type (WT) mice. The dotted line indicates the median for GPCRs expression. (B) Volcano plot for the fold change of expression level for 408 GPCRs (gray dots) in $Na_V1.8$ neurons ablated vs. control mice. Orphan receptors are shown in red with corresponding names, the size of the dots relate to the expression level prior of ablation. (C) *In situ* hybridization of selected orphan receptors (i; Gpr65 and ii; Gpr161) in red vs. immunohistochemical detection of YFP in the nodose ganglion of $Na_V1.8$ reporter mice ($Na_V1.8$-Cre-ChR2-YFP) in green. Asterisks indicate representative $Na_V1.8$ positive cells. Triangles and arrows indicate examples of orphan receptor positive cells and double positive cells, respectively.

signals act have been proven useful to our understanding of enteroendocrine cell function [66,67]. In the present study, we provide a comprehensive picture of the expression and coexpression of GPCRs in the nodose ganglion focusing on afferent vagal fibers innervating the GI tract.

The complete RNA expression profile for vagal afferent in $Na_V1.8$ ablated mice and control mice found through RNA-sequencing is given in Supplementary Table 3. It is implied that genes expressed highly in control mice and lowly after ablation are enriched in the $Na_V1.8$ fibers. However, there are potential caveats in this assumption as incomplete ablation will hinder detection for some genes, and ablation induced gene regulation could result in false positive and/or negative results. The ablation procedure has previously been shown to be very effective [44], and here we also show a strong decrease of genes specific for unmyelinated vagal afferents (Figure S1). However, we cannot rule out that some $Na_V1.8$ fibers are still present; likewise, we cannot rule out potential ablation induced gene regulation. To minimize this potential caveat, we also examined gene expression in the ganglia of wild-type mice and performed *in situ* hybridization for select receptors. Importantly, the distribution and expression levels for receptors we examined by qPCR and ISH matched very well with the data deriving from our RNAseq dataset after ablation, but these caveats should be kept in mind when interpreting our RNA sequencing dataset.

It should also be noted that transcriptional data do not always correspond to protein levels. However, it is notoriously difficult to generate specific antibodies towards GPCRs, thus hindering immunohistochemical detection. This may explain that our data are not always consistent with the literature. For instance, the ghrelin receptor has been reported to be expressed in vagal afferent using immunostaining [68]. However, our study failed to detect the ghrelin receptor mRNA. Alternatively, past studies have successfully characterized the localization and density of binding sites for several gut peptides in vagal cells using radioligands and binding assays [69,70]. However, binding assays do not allow the study of orphan receptors and are not suitable for the high-throughput screening of a large number of receptors. Hence, there are few methods available to systematically assess the protein localization and level of the receptors we identified in this study.

Many physiological studies have established that vagal afferents provide the postprandial feedback necessary for meal termination [71–73]. However, there is ongoing controversy as to the physiological importance of gut peptides signaling in vagal afferents [74]. Here we find that vagal afferents expressed relatively few, selected gut peptide receptors, which are typically low or absent in other types of peripheral afferents [75], yet abundant in GI tissues [66,67]. For instance, CCK1R and NTSR1 were enriched in vagal unmyelinated afferents, but not CCK2R, or NTS2R. Interestingly, the receptor for the other incretin hormone GIP was not expressed in afferent vagal nerves, indicating that GIP functions mainly in a classical endocrine manner. The receptor for ghrelin, a gastric hormone, which exerts its many different functions though the CNS was not expressed in vagal afferents. This supports the notion that ghrelin does not function through the afferent vagus nerve but mainly through endocrine mechanisms getting access

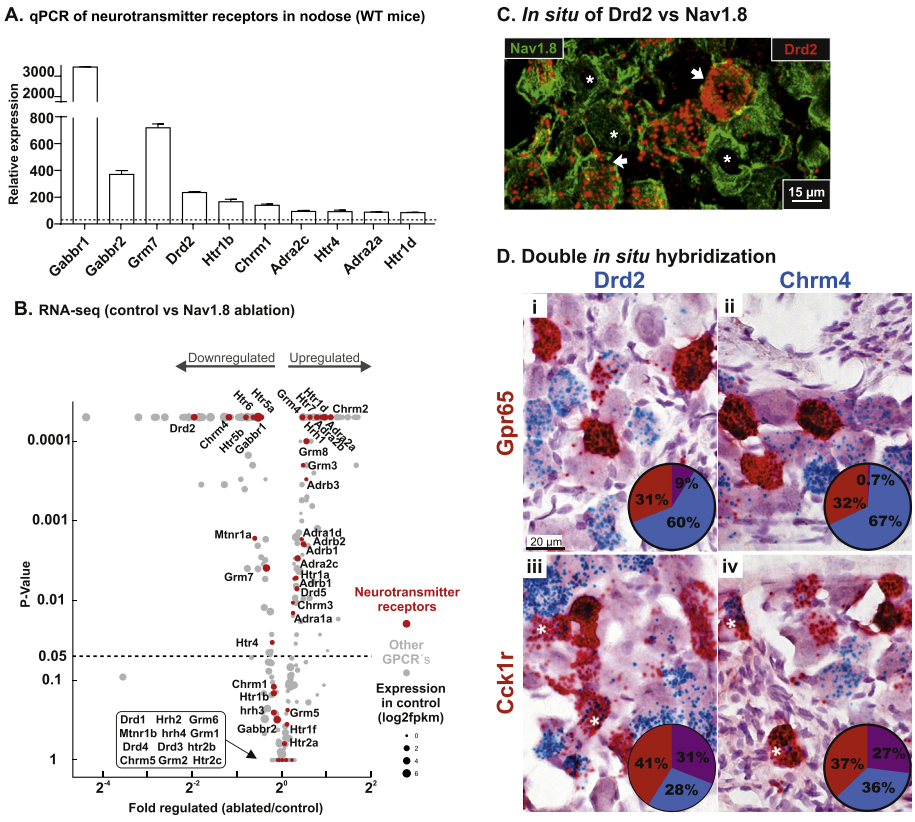

Figure 7: Neurotransmitter receptors expression and enrichment in $Na_V1.8$-expressing vagal afferents. (A) Expression level of selected neurotransmitter receptors in vagal afferent (whole nodose ganglion) of WT mice, the dotted line indicates the median for GPCRs expression. (B) Volcano plot for the fold change of expression level for 408 GPCRs (gray dots) in $Na_V1.8$ neurons ablated vs. control mice. Neurotransmitter receptors are shown in red with corresponding names, the size of the dots relate to the expression level prior of ablation. (C) *In situ* hybridization of Drd2 in red vs. immunohistochemical detection of YFP in the nodose ganglion of $Na_V1.8$ reporter mice ($Na_V1.8$-Cre-ChR2-YFP) in green. Asterisks indicate $Na_V1.8$ positive cells triangles indicate neurotransmitter receptor positive cells and arrows indicate double positive cells. (D) Double *in situ* hybridizations for-for Drd2 in blue vs. Gpr65 and Cck1r in red (i; iii) or for Chrm4 in blue vs. Gpr65 and Cck1r in red (ii; iv). Pie charts give the percentage of single positive cells (red and blue) and double positive (purple).

to ghrelin receptors in the CNS [53–55]. Thus, only four specific receptor subtypes for gut peptides were found to be enriched in vagal Nav1.8 cells and, importantly, to be coexpressed in a rather clear pattern, i.e. CCK1R together with GLP1R and the PYY Y2 receptor. In contrast, NTSR1 was expressed in another population of afferent neurons together with the orphan receptor GPR65 (Figure 8). Many of the GPR65 expressing neurons have previously been demonstrated to also express the 5-HT3 receptor, a ligand gated ion-channel activated by serotonin (5-HT) released from the enterochromaffin cells [76]. The enterochromaffin cells have further been described to potentially form "synaptic-like" contacts with fibers from the enteric nervous system and being electrically excitable with depolarization leading to serotonin release [76]. Similar "synaptic-like" contacts between enteroendocrine cells and enteric nerves have been described [77]. However, our anatomical data indicates that similar "synapse-like" contacts may not occur frequently between the axons of vagal afferents and enteroendocrine cells (Figure S6).

Consequently, neurotensin emerges as an important gut hormone with a corresponding receptor (NTSR1) preferentially expressed in the GI mucosa (paracrine function), while for the other gut hormones CCK, GLP1, and PYY the hormone has to travel further to reach a nerve with a corresponding receptor (paracrine/hormonal function). It is noteworthy that neurotensin immunoreactivity and binding sites are also very abundant in the nucleus of the solitary tract in the brain stem [70,78]. Thus, more studies are warranted to establish whether neurotensin acts on vagal terminals located either in the GI tract or the nucleus of the solitary tract. In the case of ghrelin and GIP, it appears that these must reach the CNS (classical hormone function).

The ability of unmyelinated afferents to directly respond to proinflammatory lipids has been reported in isolated vagal afferents [79,80], and it is plausible that this mechanism has been preserved during evolution with the aim of allowing peripheral sensory neurons to detect infections and tissue injuries. Here, we found that vagal afferents including those innervating the GI tract are particularly highly enriched in receptors for leukotrienes, sphingolipids, and prostaglandins (Figure 8). These receptors have been described in spinal nociceptors [75], suggesting that they play a key role in responding to noxious stimuli. However, unlike their spinal counterparts, vagal afferents, including those innervating the GI mucosa, do not convey pain [18]. Instead, we speculated that the stimulation of vagal unmyelinated afferents by inflammatory lipids would trigger an efferent response aimed at containing inflammation and maintaining tissues integrity, a biological process known as "inflammatory reflex" [81]. This hypothesis is in agreement with our data showing that unmyelinated axons in the GI mucosa are tightly associated with macrophages rather than enteroendocrine cells (Figure S6).

Receptors for several classic neurotransmitters were found to be enriched in vagal afferents including both unmyelinated and

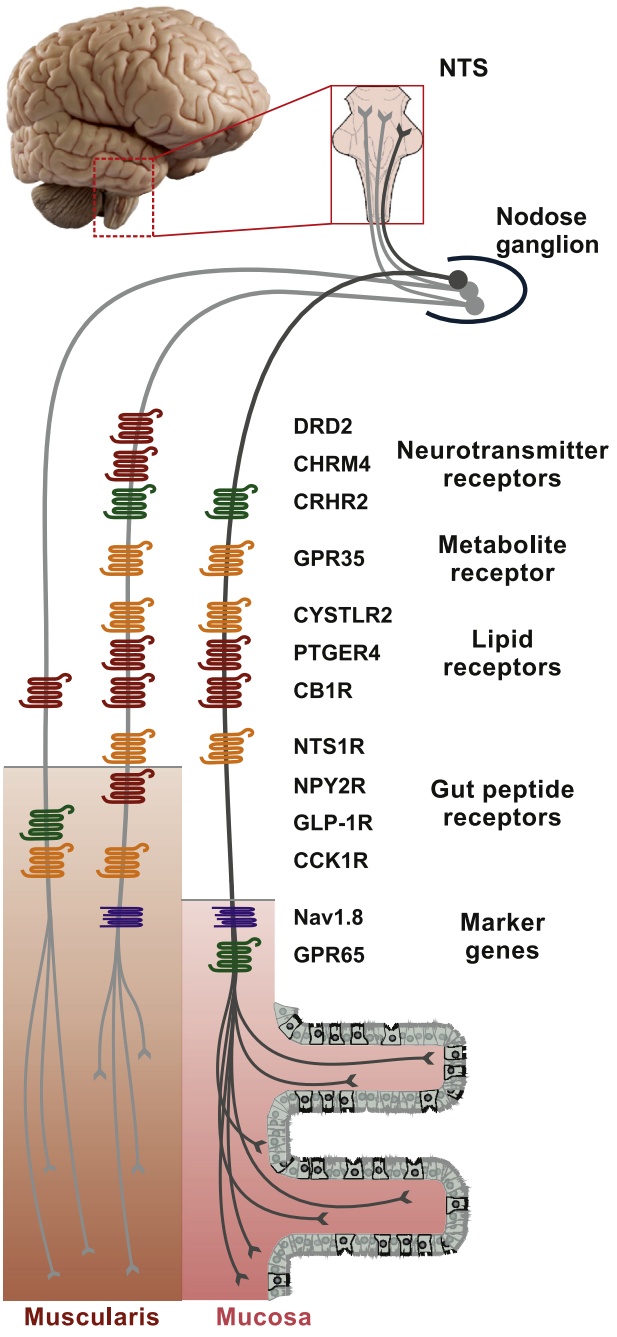

Figure 8: Schematic overview of GPCRs enriched in gastrointestinal vagal afferents. This study identified several GPCRs preferentially enriched in unmyelinated vagal afferents ($Na_v1.8$). Identified receptors encompassed a wide range of GPCRs families including receptors for neurotransmitters, metabolites, lipids, and gut peptides. We further inferred their localization in neurons projecting preferentially to either the gastrointestinal muscularis CCK1 and GLP-1 receptor expressing fibers or the mucosa GPR65 expressing fibers based on Williams and coworkers [7] and our results. Strikingly, most receptors showed a relatively widespread distribution in both categories of neurons. Receptors in green (Gαs-coupled) and orange (Gαq-coupled) are anticipated to stimulate neuronal activity. Those in red (Gαi-coupled) are anticipated to inhibit neuronal activity. Nonetheless, the downstream signaling pathways of these receptors are not known with certainty in vagal afferents. Of note, only receptors found to be mostly highly enriched in unmyelinated vagal afferents are listed here. For the purpose of simplification, orphan receptors were not indicated. NTS, nucleus of the solitary tract.

myelinated fibers. As mentioned before, mucosal 5-HT can stimulate the activity of vagal afferents [76]. However, it is unclear what could be the source(s) of the other identified neurotransmitters and neuropeptides. Hypothetically, neurotransmitters deriving from the enteric nervous system including acetylcholine and glutamate could act on vagal terminals [82]. The aforementioned neurotransmitters and peptides may also be released within the brainstem and modulate the activity of vagal afferents at the presynaptic level [65]. Hence, more studies are warranted to determine whether the receptors for neurotransmitters and neuropeptides may serve as presynaptic receptors in addition to or rather than peripheral receptors.

Vagal afferents have been proposed to serve as a relay between the GI microbiome and brain functions [83,84], presumably in response to the activation of vagal afferents by microbial metabolites. The fact that peripheral sensory neurons reside outside the blood–brain barrier makes them a particularly relevant target for pharmacological agents mimicking metabolites. Considering the well-documented interactions between microbial metabolites and GPCRs [22], we sought to examine the expression of known or proposed microbial metabolite receptors in vagal afferents. The most abundant metabolite receptor found in vagal neurons was GPR35, thus raising the possibility that vagal GPR35 signaling may be involved in the detection of aromatic acids such as the tryptophan metabolite kynureic acid (Figure 8). Interestingly, GPR35 was extensively coexpressed both with CCK1R and GPR65, two markers of GI afferents. However, surprisingly few other metabolites receptors were identified in vagal afferents, and usually at very low levels. This included FFAR3, a receptor previously described in a small subset of vagal afferents [59,60]. Importantly, intact vagal afferents were shown to be required for FFAR3 effects on metabolism [60]. It is therefore conceivable that a small number of microbiome-derived molecules may directly act on GPCRs expressed by vagal afferents. Nonetheless, most microbial metabolites are unlikely to directly target vagal afferents. Instead, they may affect afferent vagal nerves through enteroendocrine cells such as enterochomaffin cells, which are highly enriched in multiple types of receptors for microbial metabolites [85]. In summary, the unexpected identification of many GPCRs with unknown ligands and functions in vagal afferents highlights how little is known about vagal signaling. Many of the genes identified in this study may be used to generate novel transgenic mice to investigate the functional neuroanatomy of vagal afferents, for instance, using diphtheria toxin-assisted ablation tools [86] to determine their exact functions. Thus, we are hopeful that our data will guide future studies aimed at addressing the role of GPCRs signaling in visceral afferents in relation to metabolic and immune sensing, as well as metabolic diseases and their complications.

ACKNOWLEDGEMENTS

We thank Stine Lindberg Vedersø (Copenhagen) and Sarita Shah (Dallas) for expert technical assistance. The research is supported by a grant from the Danish Council for Independent Research (7016-00389A). The work on metabolite receptors is further supported by an Immunometabolism grant NNF15CC0018346 and Challenge Grants NNF15OC0016798 and NNF14OC0016798 from the Novo Nordisk Foundation. The Novo Nordisk Foundation Center for Basic Metabolic Research is supported by an unconditional grant (NNF10CC1016515).

CONFLICTS OF INTEREST

None declared.

APPENDIX A. SUPPLEMENTARY DATA

Supplementary data related to this article can be found at https://doi.org/10.1016/j.molmet.2018.03.016.

REFERENCES

[1] Palay, S.L., Karlin, L.J., 1959. An electron microscopic study of the intestinal villus. I. The fasting animal. The Journal of Biophysical Biochemical Cytology 5(3):363–372.

[2] Ushiki, T., 1992. Three-dimensional ultrastructure of the autonomic nerve terminals in the lamina propria mucosae of the rat large intestine. Archives of Histology Cytology 55(Suppl):87–94.

[3] Furness, J.B., Rivera, L.R., Cho, H.J., Bravo, D.M., Callaghan, B., 2013. The gut as a sensory organ. Nature Reviews Gastroenterology & Hepatology 10(12): 729–740.

[4] Powley, T.L., Spaulding, R.A., Haglof, S.A., 2011. Vagal afferent innervation of the proximal gastrointestinal tract mucosa: chemoreceptor and mechanoreceptor architecture. Journal of Comparative Neurology 519(4):644–660.

[5] Gautron, L., Sakata, I., Udit, S., Zigman, J.M., Wood, J.N., Elmquist, J.K., 2011. Genetic tracing of Nav1.8-expressing vagal afferents in the mouse. Journal of Comparative Neurology 519(15):3085–3101.

[6] Page, A.J., Kentish, S.J., 2014. Vagal leptin signalling: a double agent in energy homeostasis? Molecular Metabolism 3(6):593–594.

[7] Williams, E.K., Chang, R.B., Strochlic, D.E., Umans, B.D., Lowell, B.B., Liberles, S.D., 2016. Sensory neurons that detect stretch and nutrients in the digestive system. Cell 166(1):209–221.

[8] Berthoud, H.R., Patterson, L.M., 1996. Anatomical relationship between vagal afferent fibers and CCK-immunoreactive entero-endocrine cells in the rat small intestinal mucosa. Acta Anatomica 156(2):123–131.

[9] Grundy, D., 1988. Vagal control of gastrointestinal function. Baillieres Clinical Gastroenterology 2(1):23–43.

[10] Blackshaw, L.A., Grundy, D., 1990. Effects of cholecystokinin (CCK-8) on two classes of gastroduodenal vagal afferent fibre. Journal of the Autonomic Nervous System 31(3):191–201.

[11] Hillsley, K., Grundy, D., 1998. Serotonin and cholecystokinin activate different populations of rat mesenteric vagal afferents. Neuroscience Letters 255(2): 63–66.

[12] Lal, S., Kirkup, A.J., Brunsden, A.M., Thompson, D.G., Grundy, D., 2001. Vagal afferent responses to fatty acids of different chain length in the rat. American Journal of Physiology – Gastrointestinal and Liver Physiology 281(4):G907–G915.

[13] Richards, W., Hillsley, K., Eastwood, C., Grundy, D., 1996. Sensitivity of vagal mucosal afferents to cholecystokinin and its role in afferent signal transduction in the rat. The Journal of Physiology 497(Pt 2):473–481.

[14] Zhu, J.X., Zhu, X.Y., Owyang, C., Li, Y., 2001. Intestinal serotonin acts as a paracrine substance to mediate vagal signal transmission evoked by luminal factors in the rat. The Journal of Physiology 530(Pt 3):431–442.

[15] Cottrell, D.F., Iggo, A., 1984. Mucosal enteroceptors with vagal afferent fibres in the proximal duodenum of sheep. The Journal of Physiology 354:497–522.

[16] Leal-Cardoso, H., Koschorke, G.M., Taylor, G., Weinreich, D., 1993. Electrophysiological properties and chemosensitivity of acutely isolated nodose ganglion neurons of the rabbit. Journal of the Autonomic Nervous System 45(1):29–39.

[17] Iggo, A., 1957. Gastro-intestinal tension receptors with unmyelinated afferent fibres in the vagus of the cat. Quarterly Journal of Experimental Physiology & Cognate Medical Sciences 42(1):130–143.

[18] Cervero, F., 1994. Sensory innervation of the viscera: peripheral basis of visceral pain. Physiological Reviews 74(1):95–138.

[19] Janig, W., 1996. Neurobiology of visceral afferent neurons: neuroanatomy, functions, organ regulations and sensations. Biological Psychology 42(1–2): 29–51.

[20] Iggo, A., 1957. Gastric mucosal chemoreceptors with vagal afferent fibres in the cat. Quarterly Journal of Experimental Physiology & Cognate Medical Sciences 42(4):398–409.

[21] Schwartz, G.J., Moran, T.H., 1998. Duodenal nutrient exposure elicits nutrient-specific gut motility and vagal afferent signals in rat. American Journal of Physiology 274(5 Pt 2):R1236–R1242.

[22] Husted, A.S., Trauelsen, M., Rudenko, O., Hjorth, S.A., Schwartz, T.W., 2017. GPCR-mediated signaling of metabolites. Cell Metabolism 25(4):777–796.

[23] Berthoud, H.R., 2008. The vagus nerve, food intake and obesity. Regulatory Peptides 149(1–3):15–25.

[24] Ronveaux, C.C., Tome, D., Raybould, H.E., 2015. Glucagon-like peptide 1 interacts with ghrelin and leptin to regulate glucose metabolism and food intake through vagal afferent neuron signaling. Journal of Nutrition 145(4): 672–680.

[25] Kentish, S.J., Page, A.J., 2015. The role of gastrointestinal vagal afferent fibres in obesity. The Journal of Physiology 593(4):775–786.

[26] Krieger, J.P., Arnold, M., Pettersen, K.G., Lossel, P., Langhans, W., Lee, S.J., 2016. Knockdown of glp-1 receptors in vagal afferents affects normal food intake and glycemia. Diabetes 65(1):34–43.

[27] Krieger, J.P., Langhans, W., Lee, S.J., 2015. Vagal mediation of GLP-1's effects on food intake and glycemia. Physiology & Behavior 152(Pt B): 372–380.

[28] Broberger, C., Holmberg, K., Shi, T.J., Dockray, G., Hokfelt, T., 2001. Expression and regulation of cholecystokinin and cholecystokinin receptors in rat nodose and dorsal root ganglia. Brain Research 903(1-2):128–140.

[29] Nakagawa, A., Satake, H., Nakabayashi, H., Nishizawa, M., Furuya, K., Nakano, S., et al., 2004. Receptor gene expression of glucagon-like peptide-1, but not glucose-dependent insulinotropic polypeptide, in rat nodose ganglion cells. Autonomic Neuroscience 110(1):36–43.

[30] Moran, T.H., Norgren, R., Crosby, R.J., McHugh, P.R., 1990. Central and peripheral vagal transport of cholecystokinin binding sites occurs in afferent fibers. Brain Research 526(1):95–102.

[31] Nishizawa, M., Nakabayashi, H., Uchida, K., Nakagawa, A., Niijima, A., 1996. The hepatic vagal nerve is receptive to incretin hormone glucagon-like peptide-1, but not to glucose-dependent insulinotropic polypeptide, in the portal vein. Journal of the Autonomic Nervous System 61(2):149–154.

[32] Smith, G.P., Jerome, C., Cushin, B.J., Eterno, R., Simansky, K.J., 1981. Abdominal vagotomy blocks the satiety effect of cholecystokinin in the rat. Science 213(4511):1036–1037.

[33] Abbott, C.R., Monteiro, M., Small, C.J., Sajedi, A., Smith, K.L., Parkinson, J.R., et al., 2005. The inhibitory effects of peripheral administration of peptide YY(3-36) and glucagon-like peptide-1 on food intake are attenuated by ablation of the vagal-brainstem-hypothalamic pathway. Brain Research 1044(1):127–131.

[34] Ritter, R.C., Ladenheim, E.E., 1985. Capsaicin pretreatment attenuates suppression of food intake by cholecystokinin. American Journal of Physiology 248(4 Pt 2):R501–R504.

[35] Moran, T.H., Baldessarini, A.R., Salorio, C.F., Lowery, T., Schwartz, G.J., 1997. Vagal afferent and efferent contributions to the inhibition of food intake by cholecystokinin. American Journal of Physiology 272(4 Pt 2):R1245–R1251.

[36] Sisley, S., Gutierrez-Aguilar, R., Scott, M., D'Alessio, D.A., Sandoval, D.A., Seeley, R.J., 2014. Neuronal GLP1R mediates liraglutide's anorectic but not glucose-lowering effect. Journal of Clinical Investigation 124(6):2456–2463.

[37] Yamamoto, H., Kishi, T., Lee, C.E., Choi, B.J., Fang, H., Hollenberg, A.N., et al., 2003. Glucagon-like peptide-1-responsive catecholamine neurons in the area postrema link peripheral glucagon-like peptide-1 with central autonomic control sites. Journal of Neuroscience 23(7):2939–2946.

[38] Reidelberger, R.D., Hernandez, J., Fritzsch, B., Hulce, M., 2004. Abdominal vagal mediation of the satiety effects of CCK in rats. American Journal of Physiology – Regulatory, Integrative and Comparative Physiology 286(6): R1005–R1012.

[39] Schwartz, G.J., Moran, T.H., 1996. Sub-diaphragmatic vagal afferent integration of meal-related gastrointestinal signals. Neuroscience & Biobehavioral Reviews 20(1):47–56.
[40] Ripken, D., van der Wielen, N., van der Meulen, J., Schuurman, T., Witkamp, R.F., Hendriks, H.F., et al., 2015. Cholecystokinin regulates satiation independently of the abdominal vagal nerve in a pig model of total subdiaphragmatic vagotomy. Physiology & Behavior 139:167–176.
[41] Engelstoft, M.S., Egerod, K.L., Lund, M.L., Schwartz, T.W., 2013. Enteroendocrine cell types revisited. Current Opinion in Pharmacology 13(6): 912–921.
[42] Li, B.Y., Schild, J.H., 2007. Electrophysiological and pharmacological validation of vagal afferent fiber type of neurons enzymatically isolated from rat nodose ganglia. Journal of Neuroscience Methods 164(1):75–85.
[43] Schild, J.H., Kunze, D.L., 2012. Differential distribution of voltage-gated channels in myelinated and unmyelinated baroreceptor afferents. Autonomic Neuroscience 172(1–2):4–12.
[44] Udit, S., Burton, M., Rutkowski, J.M., Lee, S., Bookout, A.L., Scherer, P.E., et al., 2017. Nav1.8 neurons are involved in limiting acute phase responses to dietary fat. Molecular Metabolism 6(10):1081–1091.
[45] Yuan, X., Huang, Y., Shah, S., Wu, H., Gautron, L., 2016. Levels of Cocaine- and Amphetamine-Regulated Transcript in Vagal Afferents in the Mouse Are Unaltered in Response to Metabolic Challenges. eNeuro 3(5).
[46] Trapnell, C., Hendrickson, D.G., Sauvageau, M., Goff, L., Rinn, J.L., Pachter, L., 2013. Differential analysis of gene regulation at transcript resolution with RNA-seq. Nature Biotechnology 31(1):46–53.
[47] Roberts, A., Trapnell, C., Donaghey, J., Rinn, J.L., Pachter, L., 2011. Improving RNA-Seq expression estimates by correcting for fragment bias. Genome Biology 12(3):R22.
[48] Abrahamsen, B., Zhao, J., Asante, C.O., Cendan, C.M., Marsh, S., Martinez-Barbera, J.P., et al., 2008. The cell and molecular basis of mechanical, cold, and inflammatory pain. Science 321(5889):702–705.
[49] Usoskin, D., Furlan, A., Islam, S., Abdo, H., Lonnerberg, P., Lou, D., et al., 2015. Unbiased classification of sensory neuron types by large-scale single-cell RNA sequencing. Nature Neuroscience 18(1):145–153.
[50] Date, Y., Murakami, N., Toshinai, K., Matsukura, S., Niijima, A., Matsuo, H., et al., 2002. The role of the gastric afferent vagal nerve in ghrelin-induced feeding and growth hormone secretion in rats. Gastroenterology 123(4): 1120–1128.
[51] Burdyga, G., Varro, A., Dimaline, R., Thompson, D.G., Dockray, G.J., 2006. Ghrelin receptors in rat and human nodose ganglia: putative role in regulating CB-1 and MCH receptor abundance. American Journal of Physiology — Gastrointestinal and Liver Physiology 290(6):G1289–G1297.
[52] Grabauskas, G., Wu, X., Lu, Y., Heldsinger, A., Song, I., Zhou, S.Y., et al., 2015. KATP channels in the nodose ganglia mediate the orexigenic actions of ghrelin. The Journal of Physiology 593(17):3973–3989.
[53] Arnold, M., Mura, A., Langhans, W., Geary, N., 2006. Gut vagal afferents are not necessary for the eating-stimulatory effect of intraperitoneally injected ghrelin in the rat. Journal of Neuroscience 26(43):11052–11060.
[54] Scott, M.M., Perello, M., Chuang, J.C., Sakata, I., Gautron, L., Lee, C.E., et al., 2012. Hindbrain ghrelin receptor signaling is sufficient to maintain fasting glucose. PLoS One 7(8) e44089.
[55] Wang, Q., Liu, C., Uchida, A., Chuang, J.C., Walker, A., Liu, T., et al., 2014. Arcuate AgRP neurons mediate orexigenic and glucoregulatory actions of ghrelin. Molecular Metabolism 3(1):64–72.
[56] Williams, E.K., Chang, R.B., Strochlic, D.E., Umans, B.D., Lowell, B.B., Liberles, S.D., 2016. Sensory neurons that detect stretch and nutrients in the digestive system. Cell.
[57] Chang, R.B., Strochlic, D.E., Williams, E.K., Umans, B.D., Liberles, S.D., 2015. Vagal sensory neuron subtypes that differentially control breathing. Cell 161(3): 622–633.
[58] Grunddal, K.V., Ratner, C.F., Svendsen, B., Sommer, F., Engelstoft, M.S., Madsen, A.N., et al., 2016. Neurotensin is coexpressed, coreleased, and acts together with GLP-1 and PYY in enteroendocrine control of metabolism. Endocrinology 157(1):176–194.
[59] Nohr, M.K., Egerod, K.L., Christiansen, S.H., Gille, A., Offermanns, S., Schwartz, T.W., et al., 2015. Expression of the short chain fatty acid receptor GPR41/FFAR3 in autonomic and somatic sensory ganglia. Neuroscience 290: 126–137.
[60] De Vadder, F., Kovatcheva-Datchary, P., Goncalves, D., Vinera, J., Zitoun, C., Duchampt, A., et al., 2014. Microbiota-generated metabolites promote metabolic benefits via gut-brain neural circuits. Cell 156(1–2):84–96.
[61] Randich, A., Tyler, W.J., Cox, J.E., Meller, S.T., Kelm, G.R., Bharaj, S.S., 2000. Responses of celiac and cervical vagal afferents to infusions of lipids in the jejunum or ileum of the rat. American Journal of Physiology — Regulatory, Integrative and Comparative Physiology 278(1):R34–R43.
[62] Ho, C.Y., Gu, Q., Hong, J.L., Lee, L.Y., 2000. Prostaglandin E(2) enhances chemical and mechanical sensitivities of pulmonary C fibers in the rat. American Journal of Respiratory and Critical Care Medicine 162(2 Pt 1):528–533.
[63] Lin, Y.S., Lee, L.Y., 2002. Stimulation of pulmonary vagal C-fibres by anandamide in anaesthetized rats: role of vanilloid type 1 receptors. The Journal of Physiology 539(Pt 3):947–955.
[64] Furness, J.B., 2012. The enteric nervous system and neurogastroenterology. Nature Reviews Gastroenterology & Hepatology 9(5):286–294.
[65] Tan, L.A., Vaughan, J.M., Perrin, M.H., Rivier, J.E., Sawchenko, P.E., 2017. Distribution of corticotropin-releasing factor (CRF) receptor binding in the mouse brain using a new, high-affinity radioligand, [125 I]-PD-Sauvagine. Journal of Comparative Neurology 525(18):3840–3864.
[66] Engelstoft, M.S., Park, W.M., Sakata, I., Kristensen, L.V., Husted, A.S., Osborne-Lawrence, S., et al., 2013. Seven transmembrane G protein-coupled receptor repertoire of gastric ghrelin cells. Molecular Metabolism 2(4):376–392.
[67] Egerod, K.L., Engelstoft, M.S., Grunddal, K.V., Nohr, M.K., Secher, A., Sakata, I., et al., 2012. A major lineage of enteroendocrine cells coexpress CCK, secretin, GIP, GLP-1, PYY, and neurotensin but not somatostatin. Endocrinology 153(12):5782–5795.
[68] Heldsinger, A., Grabauskas, G., Wu, X., Zhou, S., Lu, Y., Song, I., et al., 2014. Ghrelin induces leptin resistance by activation of suppressor of cytokine signaling 3 expression in male rats: implications in satiety regulation. Endocrinology 155(10):3956–3969.
[69] Zarbin, M.A., Wamsley, J.K., Innis, R.B., Kuhar, M.J., 1981. Cholecystokinin receptors: presence and axonal flow in the rat vagus nerve. Life Sciences 29(7):697–705.
[70] Kessler, J.P., Beaudet, A., 1989. Association of neurotensin binding sites with sensory and visceromotor components of the vagus nerve. Journal of Neuroscience 9(2):466–472.
[71] Powley, T.L., Phillips, R.J., 2004. Gastric satiation is volumetric, intestinal satiation is nutritive. Physiology & Behavior 82(1):69–74.
[72] Fox, E.A., Phillips, R.J., Martinson, F.A., Baronowsky, E.A., Powley, T.L., 2000. Vagal afferent innervation of smooth muscle in the stomach and duodenum of the mouse: morphology and topography. Journal of Comparative Neurology 428(3):558–576.
[73] Fox, E.A., Phillips, R.J., Baronowsky, E.A., Byerly, M.S., Jones, S., Powley, T.L., 2001. Neurotrophin-4 deficient mice have a loss of vagal intraganglionic mechanoreceptors from the small intestine and a disruption of short-term satiety. Journal of Neuroscience 21(21):8602–8615.
[74] Berthoud, H.R., 2008. Vagal and hormonal gut-brain communication: from satiation to satisfaction. Neuro-Gastroenterology and Motility 20(Suppl. 1):64–72.
[75] Chiu, I.M., Barrett, L.B., Williams, E.K., Strochlic, D.E., Lee, S., Weyer, A.D., et al., 2014. Transcriptional profiling at whole population and single cell levels reveals somatosensory neuron molecular diversity. Elife 3.

[76] Bellono, N.W., Bayrer, J.R., Leitch, D.B., Castro, J., Zhang, C., O'Donnell, T.A., et al., 2017. Enterochromaffin cells are gut chemosensors that couple to sensory neural pathways. Cell 170(1), 185–198 e16.

[77] Bohorquez, D.V., Chandra, R., Samsa, L.A., Vigna, S.R., Liddle, R.A., 2011. Characterization of basal pseudopod-like processes in ileal and colonic PYY cells. Journal of Molecular Histology 42(1):3–13.

[78] Emson, P.C., Goedert, M., Horsfield, P., Rioux, F., St Pierre, S., 1982. The regional distribution and chromatographic characterisation of neurotensin-like immunoreactivity in the rat central nervous system. Journal of Neurochemistry 38(4):992–999.

[79] Kwong, K., Lee, L.Y., 2005. Prostaglandin E2 potentiates a TTX-resistant sodium current in rat capsaicin-sensitive vagal pulmonary sensory neurones. The Journal of Physiology 564(Pt 2):437–450.

[80] Cordoba-Rodriguez, R., Moore, K.A., Kao, J.P., Weinreich, D., 1999. Calcium regulation of a slow post-spike hyperpolarization in vagal afferent neurons. Proceedings of the National Academy of Sciences of the U S A 96(14): 7650–7657.

[81] Andersson, U., Tracey, K.J., 2012. Reflex principles of immunological homeostasis. Annual Review of Immunology 30:313–335.

[82] Liu, M.T., Rothstein, J.D., Gershon, M.D., Kirchgessner, A.L., 1997. Glutamatergic enteric neurons. Journal of Neuroscience 17(12):4764–4784.

[83] Liao, W.H., Henneberg, M., Langhans, W., 2016. Immunity-based evolutionary interpretation of diet-induced thermogenesis. Cell Metabolism 23(6):971–979.

[84] Dinan, T.G., Stilling, R.M., Stanton, C., Cryan, J.F., 2015. Collective unconscious: how gut microbes shape human behavior. Journal of Psychiatric Research 63:1–9.

[85] Lund, M.L., Egerod, K.L., Engelstoft, M.S., Dmytriyeva, O., Theodorsson, E., Patel, B.A., et al., 2018. Enterochromaffin 5-HT cells - a major target for GLP-1 and gut microbial metabolites. Molecular Metabolism. https://doi.org/10.1016/j.molmet.2018.03.004. Accepted.

[86] Pereira, M.M., Mahu, I., Seixas, E., Martinez-Sanchez, N., Kubasova, N., Pirzgalska, R.M., et al., 2017. A brain-sparing diphtheria toxin for chemical genetic ablation of peripheral cell lineages. Nature Communications 8:14967.

